Journal of Applied Polymer Science

Mechanical and thermal properties of poly(butylene succinate)/poly(3-hydroxybutyrate-*co*-3-hydroxyvalerate) biodegradable blends

Y. J. Phua,[1,2] A. Pegoretti,[3] T. Medeiros Araujo,[3] Z. A. Mohd Ishak[1,4]

[1]Cluster for Polymer Composites, Science and Engineering Research Centre, Engineering Campus, Universiti Sains Malaysia, Nibong Tebal 14300, Penang, Malaysia

[2]Physics of Geological Processes, Department of Physics, University of Oslo, P.O. Box 1048 Blindern, Oslo 0316, Norway

[3]Department of Industrial Engineering, University of Trento, Trento 38123, Italy

[4]School of Materials and Mineral Resources Engineering, Universiti Sains Malaysia, Nibong Tebal 14300, Penang, Malaysia

Correspondence to: Z. A. Mohd Ishak (E-mail: zarifin@eng.usm.my or zarifin.ishak@gmail.com)

ABSTRACT: Biodegradable polymer blends of poly(butylene succinate) (PBS) and poly(3-hydroxybutyrate-*co*-3-hydroxyvalerate) (PHBV) were prepared with different compositions. The mechanical properties of the blends were studied through tensile testing and dynamic mechanical thermal analysis. The dependence of the elastic modulus and strength data on the blend composition was modeled on the basis of the equivalent box model. The fitting parameters indicated complete immiscibility between PBS and PHBV and a moderate adhesion level between them. The immiscibility of the parent phases was also evidenced by scanning electron observation of the prepared blends. The thermal properties of the blends were studied through differential scanning calorimetry (DSC) and thermogravimetric analysis (TGA). The DSC results showed an enhancement of the crystallization behavior of PBS after it was blended with PHBV, whereas the thermal stability of PBS was reduced in the blends, as shown by the TGA thermograms. © 2015 Wiley Periodicals, Inc. J. Appl. Polym. Sci. **2015**, *132*, 42815.

KEYWORDS: biodegradable; biopolymers and renewable polymers; blends; mechanical properties; thermal properties

Received 17 January 2015; accepted 6 August 2015

DOI: 10.1002/app.42815

INTRODUCTION

Because of increasing concerns about the fast depletion of traditional sources of fossil fuels and environmental pollution by plastic wastes, the global trend toward replacing conventional nondegradable polymers with biodegradable ones has grown at a fast pace in recent years. According to a comprehensive global report released by Global Industry Analysts,[1] the global market for biodegradable polymers will continue to expand, and it is expected to reach 825,000 tons by the year 2015. Some of the most important and most widely used biodegradable polymers are thermoplastic polyesters, such as poly(lactic acid), poly(butylene succinate) (PBS), and polyhydroxyalkanoate.[2]

PBS is a biodegradable synthetic aliphatic polyester synthesized by the polycondensation of 1,4-butanediol and succinic acid and was invented in the early 1990s by Showa Highpolymer in Japan. It exhibits superior mechanical and thermal properties, high chemical resistance, great availability, and lower material cost over other biodegradable polymers.[3–5] However, the production of PBS involves poly(alkylene succinate), which is synthesized from petrochemical precursors. Manufacturers are developing the production of PBS with biobased succinic acid for the synthesis of PBS, but synthetic PBS is still more common in the market. Therefore, blending synthetic PBS with other biobased materials is another option for replacing a fraction of PBS with a more environmentally friendly material, and it offers us the possibility of modifying or tuning its properties.

The objective of this research was to investigate the microstructure and thermomechanical properties of blends between PBS and another biobased polymer, that is, poly(3-hydroxybutyrate-*co*-3-hydroxyvalerate) (PHBV). PHBV is a family of polyhydroxyalkanoates, which are fully biobased and biodegradable polymers.[6,7] PHBV is a brittle plastic with a high modulus value, low elongation at break, and poor thermal resistance.[8] On the other hand, PBS is a softer material with a relatively low modulus and a higher elongation at break and thermal stability.[9] Therefore, the blending of PBS and PHBV offers us the possibility of combining the advantages of these polymers while simultaneously mitigating their less desirable properties.

To the best of our knowledge, research on biodegradable blends based on PBS and PHBV has not been extensively reported in the open scientific literature.[10–15] The miscibility and crystallization behavior of PBS/PHBV blends at different

Table I. Material Designations and Blend Compositions

Material designation	Composition	Parts
PBS	PBS	100
PHBV	PHBV	100
90 : 10	PBS/PHBV	90 : 10
70 : 30	PBS/PHBV	70 : 30
50 : 50	PBS/PHBV	50 : 50

compositions in the range from 80 : 20 to 20 : 80 was investigated by Qiu *et al.*[12] on PHBV with a 3-hydroxyvalerate content of 14 mol %. According to their findings, PBS was immiscible with PHBV, which was inferred from the independence of the glass-transition temperature (T_g) and the phase-separated melt. Ma *et al.*[11] reported on the toughening of PHBV/PBS and blends via *in situ* compatibilization with dicumyl peroxide as a free-radical grafting initiator. In the aforementioned research, a PHBV with a 3-hydroxyvalerate content of 1 mol % was used. In this study, we selected a PHBV with 5 mol % 3-hydroxyvalerate as an attempt to study the effects of the PHBV composition on the properties of the PBS/PHBV blends. Previous work on PBS/PHBV blends has mainly focused on investigating the miscibility and crystallization behavior of the blends. However, little attention has been paid to the study of the mechanical and thermomechanical properties of the blends. Therefore, in this study, we focused our attention on the mechanical and thermal properties of PBS/PHBV blends with various compositions and with PBS as the dominant phase.

EXPERIMENTAL

Materials

PBS (Bionolle #1020), with a melting temperature of 115°C and a density of 1.26 g/cm^3, was obtained from Showa Highpolymer Co., Ltd. (Tokyo). PHBV (Enmat Y1000), with a melting temperature of 175°C, a density of 1.25 g/cm^3, and a 3-hydroxyvalerate content of 5 mol %, was supplied by Ningbo Tianan Biologic Material Co., Ltd.

Blend Preparation

PBS and PHBV pellets were dried overnight at 80°C in a vacuum oven. PBS/PHBV blends with different compositions (see Table I) were prepared by melt blending in an internal mixer (Rheomix 600, Thermo Haake, Karlsruhe, Germany) with counterrotating roller rotors. First, PHBV was fed into the mixer and mixed for 3 min at a temperature of 190°C and with a rotor speed of 60 rpm. Subsequently, PBS was added, and the blends were mixed for another 5 min. Then, square sheets with 1 mm thicknesses were produced by compression molding with a Carver hydraulic laboratory press at 190°C; this was followed by fast cooling. ISO 527 1BA tensile specimens were punch-cut from the obtained sheets.

Scanning Electron Microscopy (SEM)

The samples were fractured in liquid nitrogen, and the fracture surfaces were observed with a Zeiss Supra 40 (Carl Zeiss, Berlin, Germany) field emission scanning electron microscope at an accelerating voltage of 3 kV. Before the observations, the samples were sputter-coated with a thin layer of gold to prevent electrical charging during examination.

Differential Scanning Calorimetry (DSC)

DSC analysis was carried out with a DSC-30 calorimeter (Mettler Toledo, Langacher Greifensee Switzerland) under a nitrogen flow. The sample was heated from −70 to 200°C at a heating rate of 10°C/min and held at 200°C for 3 min. The sample was then cooled from 200 to −70°C at the same heating rate. Next, a second heating scan was performed from −70 to 200°C. The degree of crystallinity of the PBS ($\chi_{c,1}$) and the degree of crystallinity of the PHBV ($\chi_{c,2}$) phases were estimated with the following equation:[16]

$$\chi_c = \frac{\Delta H_m}{\Delta H_m^0 \times w} \times 100\% \quad (1)$$

where χ_c is the degree of crystallinity, ΔH_m is the melting enthalpy of the sample, ΔH_m^0 is the melting enthalpy of the 100% crystalline PBS (110.3 J/g)[17] or PHBV (146.6 J/g),[18] and w is the weight fraction of the PBS or PHBV in the blends.

Thermogravimetric Analysis (TGA)

TGA was performed with a TGA Q5000 analyzer (TA Instruments, New Castle, DE) under a nitrogen atmosphere from room temperature to 700°C at a heating rate of 20°C/min.

Tensile Testing

Tensile tests were performed on ISO 527-2 type 1BA specimens with an Instron model 4502 universal testing machine (Norwood, MA) equipped with a 10-kN load cell. An extensometer (Instron model 2620) with a gauge length of 12.5 mm was attached to the specimens to measure the strain values up to 2% at a crosshead speed of 1 mm/min. According to ISO 527, the elastic modulus was evaluated as a secant value between deformation levels of 0.05 and 0.25%. Tensile testing up to fracture was performed at a higher crosshead speed (10 mm/min) without the extensometer. Tests were performed at room temperature on five specimens for each sample.

Dynamic Mechanical Thermal Analysis (DMTA)

DMTA testing under tensile configuration was carried out with a DMA Q800 instrument (TA Instruments, New Castle, DE) on rectangular strips with dimensions of 15 × 5 × 1 mm^3. Testing was performed in a temperature range of −100 to 110°C at a frequency of 1 Hz.

RESULTS AND DISCUSSION

Microstructure

The SEM micrographs of the cryofractured cross-sectional surfaces of the PBS/PHBV blends are shown in Figure 1. A clear phase separation was observed on the fractured surface of all of the investigated blends, with PBS as the continuous phase and PHBV as the dispersed phase. This suggested a poor compatibility between the PBS and PHBV phases. Similar observations were reported by Ma *et al.*[11] and Qiu *et al.*,[15] who found that PBS and PHBV showed virtually no miscibility with each other. As shown in Figure 1, the dispersed phase became larger as the PHBV content increased in the blends. In the 90 : 10 blend, PHBV assumed the shape of small particles in the blend with

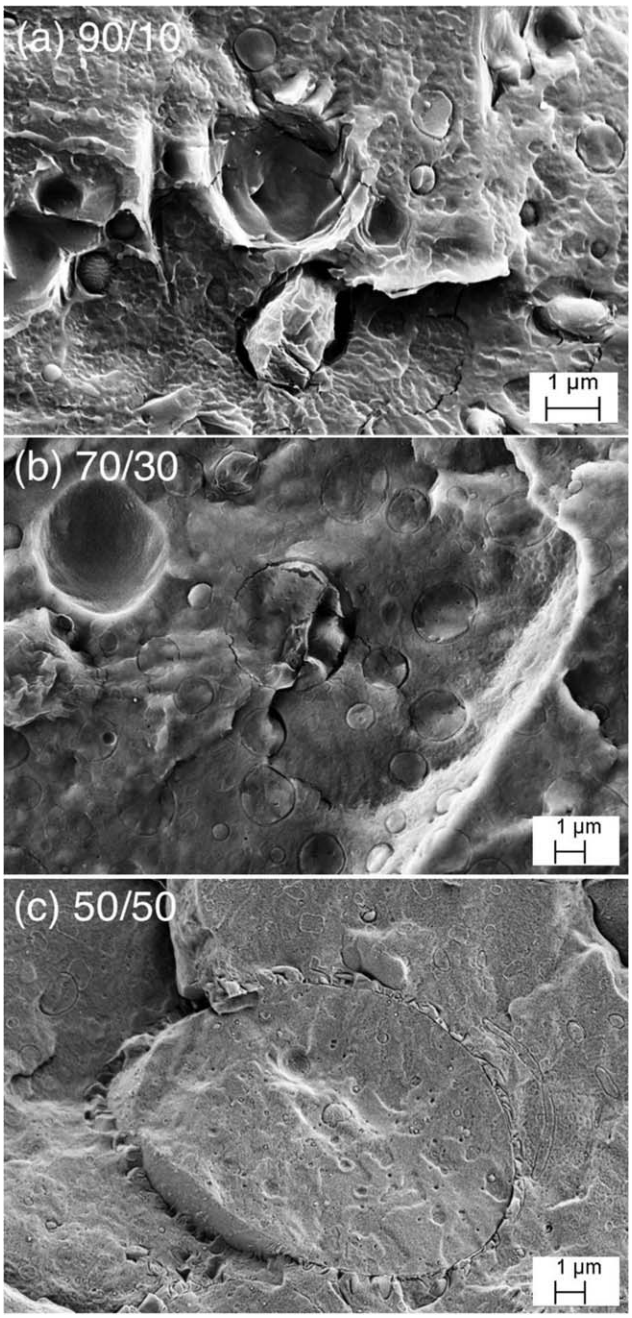

Figure 1. SEM micrographs of the (a) 90 : 10, (b) 70 : 30, and (c) 50 : 50 blends.

diameters of about 0.4–1.3 μm. In the 70 : 30 blends, the size of the PHBV phase increased to diameters of about 0.5–4.7 μm. In addition, traces of debonding of the PHBV phase were also detected from the micrographs, with some visible holes on the fracture surface. It was difficult to differentiate between the PBS and PHBV phases in the 50 : 50 blend [Figure 1(c)], but a clear phase separation was noticeable.

The interfaces of immiscible polymer blends such as PBS/PHBV play an important role in determining the kinetics of phase separation and their physical and mechanical properties. A compatible polymer blend is able to form adhesive bonds by means of interdiffusion of molecules across the interface of both phases.[19] Good adhesion can be obtained when the molecules diffuse enough to create entanglements on both sides of the interfaces.[20] From the SEM micrographs, it was obvious that the interfacial adhesion between PBS and PHBV was poor, with visible gaps at the interfaces of both phases. This means that they were incompatible, the mutual diffusion was limited, and the bond strength was low. This was due to lack of functional groups in the chemical compositions of PBS and PHBV that allowed them to interact and form interfacial chemical bonds. Two possible strategies for improving the adhesion at incompatible interfaces are the addition of compatibilizers, such as grafted or block polymers, and the formation of reactive bonding by an *in situ* reaction during the blending process.[11]

On the other hand, the fractured surface showed that the PBS/PHBV blends became more brittle as the PHBV content increased in the blend. The fractured surface of the 90 : 10 blend showed some features of ductile materials, with larger necking regions and an overall rougher appearance. This revealed that a certain degree of yielding occurred. These features became less obvious in the 70 : 30 blend but were still noticeable in a certain area of the fractured surface. For the 50 : 50 blend, a smooth and clear fractured surface was detected; this indicated that the material failed in a brittle manner.

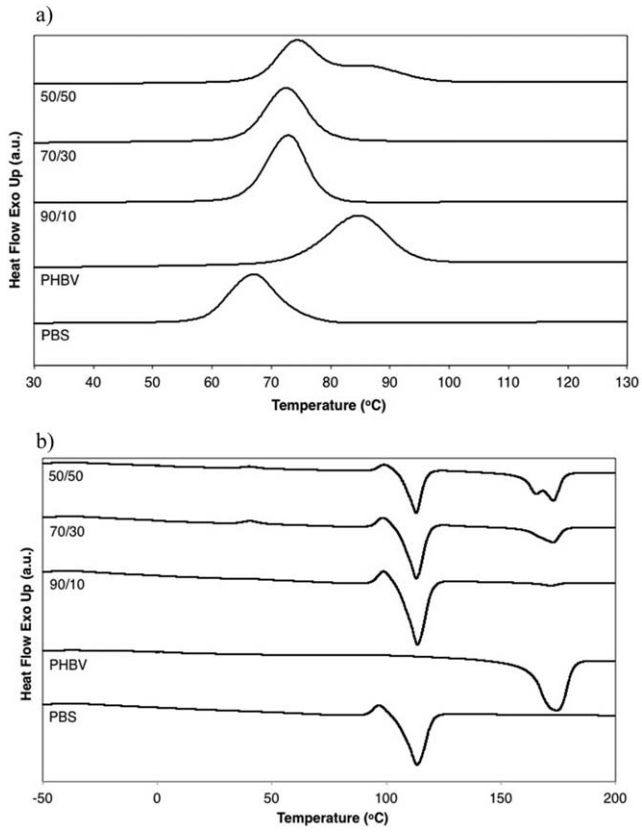

Figure 2. DSC thermograms: (a) cooling scan after melting and (b) second heating scan.

Table II. DSC Results for PBS, PHBV, and Their Blends

Compound	T_c (°C)	$T_{m,1}$ (°C)	$T_{m,2}$ (°C)	$H_{f,1}$ (J/g)	$H_{f,2}$ (J/g)	$\chi_{c,1}$ (%)	$\chi_{c,2}$ (%)
PBS	67.0	113.4	—	68.7	—	62.3	—
PHBV	84.7	—	174.5	—	85.5	—	58.3
90 : 10	72.8	113.5	171.9	79.3	2.2	79.9	15.0
70 : 30	72.4	113.1	172.7	59.5	19.3	77.1	43.9
50 : 50	74.4	112.9	172.8	40.5	40.7	73.4	55.5

T_{dmax}, maximum decomposition temperature.$T_{m,1}$, lower melting peak; $T_{m,2}$, higher melting peak; $T_{f,1}$, enthalpy of fusion for the lower melting peak; $T_{f,2}$, enthalpy of fusion for the higher melting peak.

Thermal Analysis (DSC and TGA)

To erase any possible interference of the previous thermal history, the first heating scan was disregarded, and the analyses were focused on the data obtained during the cooling and second heating scans performed after the first scan and the permanence of the sample at 200°C for 3 min. The DSC thermograms measured during the cooling scan after melting and the second heating scan of PBS, PHBV, and the blends are depicted in Figure 2. The main quantities detectable from the DSC scans are summarized in Table II. It is important to underline that for semicrystalline polymers such as PBS and PHBV, T_g is often hardly detectable on DSC thermograms because of the large portion of the crystalline region in the materials. In fact, in our DSC analyses, T_g was not visible in the DSC scans, even when a relatively high rate was adopted in the cooling scans to increase the portion of the amorphous region. Therefore, in this study, DSC analysis was only used to study the thermal behavior of the blends, whereas T_g was investigated through DMTA, as discussed in the last section of this article.

The crystallization behaviors of PBS, PHBV, and their blends are shown in Figure 2(a). The crystallization temperatures (T_c's) of the neat PBS and PHBV were located around 67 and 87°C, respectively. Only one crystallization peak was observed in each of the 90 : 10 and 70 : 30 blends, with a T_c around 72°C. This seemed to indicate that the presence of a large amount of PBS partially hindered the crystallization of the PHBV phase, at least to a PBS/PHBV ratio of 70 : 30. The DSC cooling scans also indicated the appearance of a small shoulder around 85–90°C in the 50 : 50 blend; this was related to the crystallization of PHBV. On the other hand, the T_c of PBS was increased by 4–5°C in the blends as compared to its original peak position (67°C). This showed that the presence of PHBV enhanced the crystallization rate of PBS. We believe that the presence of PHBV may have restricted the motion of PBS molecular chains and thus favored their packing and crystallization.

From the second heating scans reported in Figure 2(b), we clearly noticed that two melting peaks were identified in all of the blends; these correspond to the melting peaks of PBS and PHBV. The intensity of the peaks increased with their content in the blend. The blending of PBS and PHBV did not induce a significant change in the melting temperature (T_m) of PBS. The T_m of PHBV decreased slightly by about 2°C; this was due to the recrystallization process, which caused a slight shift in T_m. For the 50 : 50 blend, an additional peak appeared in the DSC melting scans at about 163°C. This was believed to be the melting peak of 3-hydroxyvalerate constituents in the PHBV copolymer. This peak was not visible in the heating scan of the neat PHBV because it was masked by the melting peak of poly(3-hydroxybutyrate); this caused a broader melting peak. The previous observations were in good agreement with those previously reported by Qiu *et al.*[21] and Ma *et al.*[11]

The obtained results are presented in Table II. Neat PBS exhibited a crystallinity degree of 62.3%, which was higher than that of PHBV (58.3%). In the blends, the degree of crystallinity of PBS was higher than that of PBS alone. An opposite trend was observed for the PHBV phase in the blends, where the degree of crystallinity was lower than that of the neat polymer. Furthermore, the degree of crystallinity of each phase increased with its

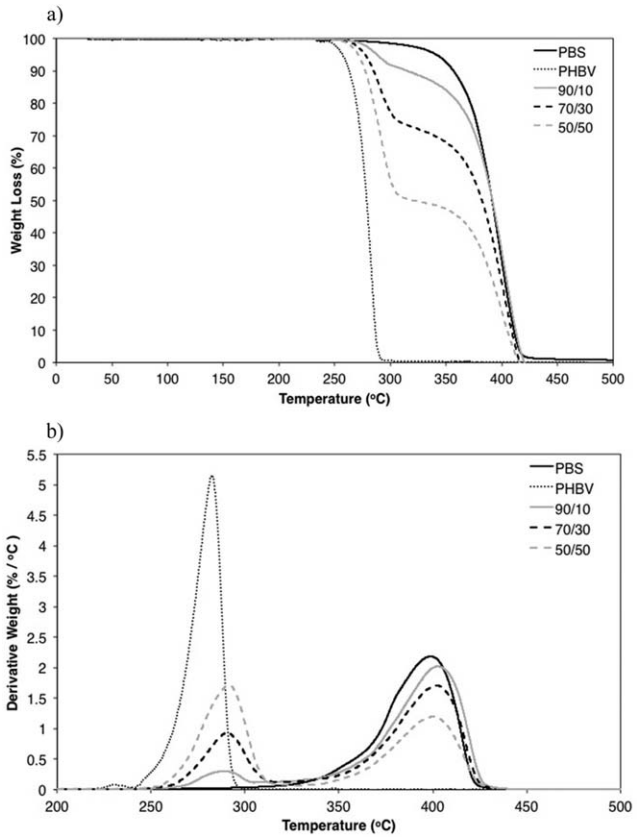

Figure 3. TGA thermograms of PBS, PHBV, and their blends: (a) weight loss and (b) derivative weight loss curves.

Table III. Thermal Stability of PBS, PHBV, and Their Blends

Compound	$T_{dmax,1}$ (°C)	$T_{dmax,2}$ (°C)
PBS	—	423.6
PHBV	282.5	—
90 : 10	288.0	402.8
70 : 30	290.9	403.0
50 : 50	291.5	399.8

T_{dmax}, maximum decomposition temperature.

content in the blends. Thus, we concluded that the blending of PBS and PHBV had positive effects on the crystallization of PBS, whereas the presence of PBS partially suppressed the crystal growth of PHBV.

Figure 3(a) shows the weight loss curves of PBS, PHBV, and their blends. The TGA curves of the neat PBS and PHBV displayed single-stage degradation processes around 300–400 and 230–300°C, respectively; these corresponded to the structural decomposition of the polymers. The 3-hydroxyvalerate content in PHBV was too low (5 mol %) and hardly detectable from the TGA curves. We observed that PBS and PHBV exhibited almost 100% weight loss after decomposition. Two distinct degradation stages were detected on the TGA curves of the PBS/PHBV blends. The first degradation stage at lower temperature corresponded to the decomposition of PHBV, whereas the second degradation stage at higher temperature corresponded to the decomposition of PBS. Thereby, the contents of PBS and PHBV phase in the blends could be estimated. The first degradation stages of the 90 : 10, 70 : 30, and 50 : 50 blends accounted for weight losses of around 10, 26, and 49%, respectively; these roughly corresponded to the PHBV contents in the blends.

The maximum decomposition temperature could be estimated at the temperature corresponding to the maximum degradation rate on the weight loss curve. The maximum decomposition temperature could be clearly located through the derivative of the weight loss curves reported in Figure 3(b). The results, presented in Table III, show that PBS had a higher thermal stability than PHBV. Nevertheless, after blending with PBS, the thermal stability of PHBV was slightly improved, whereas the thermal

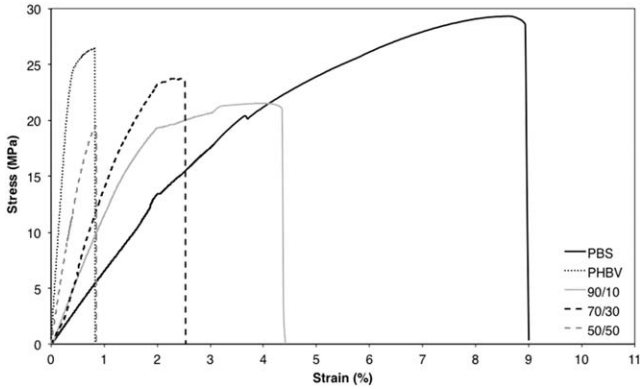

Figure 4. Typical stress–strain curves of PBS, PHBV, and their blends.

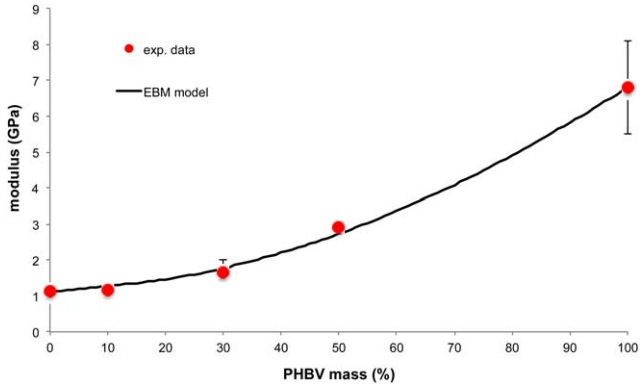

Figure 5. Effect of the PHBV content on E_b of the PBS/PHBV blends. The solid line represents the predictions of eq. (A-) in Appendix A with the universal input parameters $v_{1cr} = v_{2cr} = 0.16$ and $q_1 = q_2 = 1.8$. [Color figure can be viewed in the online issue, which is available at wileyonlinelibrary.com.]

stability of PBS was reduced. This was in agreement with the observations reported by Zhu *et al.*,[13] who also found that the blending of PBS with PHBV led to an enhancement in the thermal stability of the PHBV phase. We believe that the interactions of the PBS and PHBV molecular chains retarded the degradation of PHBV to a certain degree. At the same time, the less thermally stable PHBV also caused a reduction in the thermal stability of PBS.

Mechanical Properties

Representative tensile stress–strain curves of the neat PBS and PHBV and their relative blends are reported in Figure 4. From a direct comparison of the stress–strain curves, it clearly emerged that PBS is a soft material with a relatively low modulus value. After blending with PHBV, the tensile modulus increased because of the contribution of the high-modulus PHBV.

The trend of the tensile modulus values is plotted in Figure 5 as a function of the material composition. Generally, the mechanical properties of polymer blends can be predicted with numerous theoretical models, such as the equivalent box model (EBM), lattice spring model, Halpin Tsai equation, and Kerner's model.[22,23] In this study, the experimental values of the tensile modulus data were modeled with the EBM scheme originally proposed by Kolarik for binary polymer blends.[24–31] This approach is schematically described in Appendix A, in which the relevant literature is also cited. Because of the very small differences between the densities of PBS and PHBV (1.25 vs 1.26 g/cm^3), at first approximation, the volume fraction of a blend was taken to be equal to the weight fraction. It is worthwhile to note that the tensile modulus data could be fitted very well by the feeding of the model with the universal parameters derived from percolation theory. This experimental evidence confirmed the complete immiscibility of the two investigated polymers.

The tensile strength data of the neat polymers and relative blends are summarized in Figure 6. Both neat PBS and PHBV showed similar tensile strengths (~29 MPa). A significant reduction in the tensile strength was observed in their blends.

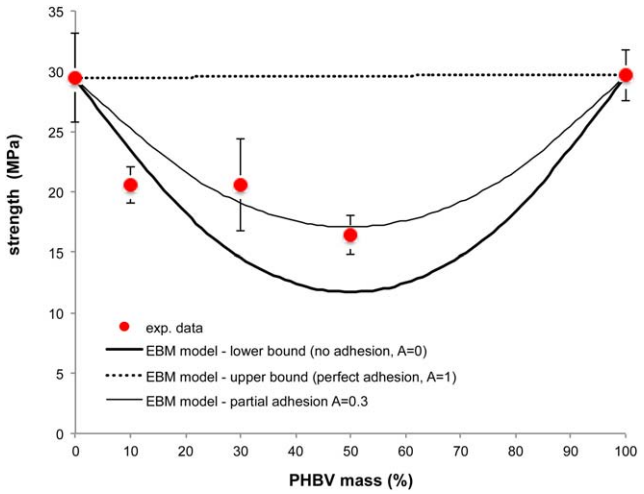

Figure 6. Effect of the PHBV content on the tensile strength of the PBS/PHBV blends. The lines represent the predictions of eq. (A-) in Appendix A with the universal input parameters $v_{1cr} = v_{2cr} = 0.16$ and $q_1 = q_2 = 1.8$ and various *A*s. [Color figure can be viewed in the online issue, which is available at wileyonlinelibrary.com.]

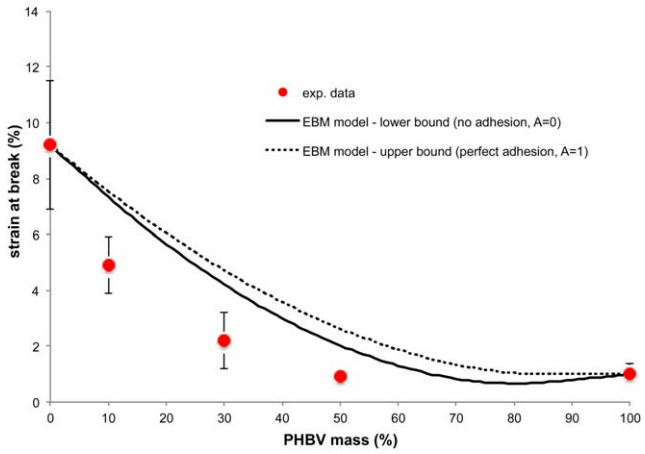

Figure 7. Effect of the PHBV content on the tensile strain at break of the PBS/PHBV blends. The lines represent the predictions of eq. (A-) in Appendix A with the universal input parameters $v_{1cr} = v_{2cr} = 0.16$ and $q_1 = q_2 = 1.8$ and two extreme *A*s. [Color figure can be viewed in the online issue, which is available at wileyonlinelibrary.com.]

The 90 : 10 and 70 : 30 blends showed similar tensile strengths around 20 MPa, whereas the 50 : 50 blend exhibited a 20.4% lower strength than the other blends. The poor tensile strength of the blends was mainly attributed to the poor interactions between PBS and PHBV from the formation of the immiscible blend. It was interesting to observe that also these experimental data fit very well with the EBM model. The continuous and dotted lines plotted in Figure 6 represent the predictions of eq. (A-) in Appendix A with the universal input parameters $v_{1cr} = v_{2cr} = 0.16$, where v_{1cr} and v_{2cr} are the critical volume fractions (the percolation thresholds) at which components 1 and 2, respectively, become partially continuous; $q_1 = q_2$ 1.8, where q_1 and q_2 are the critical exponents of components 1 and 2, respectively; and various levels of interfacial bonding (*A*s). The best fitting could be obtained with an *A* value of 0.3, which represents a relatively low *A*. Because of the poor interfacial adhesion between PBS and PHBV, the applied stress could not be effectively transferred to the dispersed PHBV phase via the interface. This behavior could be correlated with the observations previously reported on SEM and DSC data.

The strain at break (reported in Figure 7) decreased drastically as the fraction of PHBV in the blends increased. The brittle behavior of PHBV with an elongation at break of lower than 1% was clearly indicated by the typical stress–strain curves, as presented in Figure 4. Hence, the presence of PHBV in the blends gave a negative effect on the ductility of the blends. Also, we believe that the poor compatibility between PBS/PHBV also resulted in the low elongation at break of the blends. On the other hand, PBS exhibited semiductile fracture behavior, with yielding of the material detected on the stress–strain curves. This was also well reported in our previous publication.[32] EBM with universal input parameters $v_{1cr} = v_{2cr} = 0.16$ and $q_1 = q_2 = 1.8$ was capable of qualitatively following the experimental data, but the estimated trend did not properly fit the experimental points. The EBM model is based on the constancy of the properties of the neat components (in this case, PBS and PHBV) in the polymer blends. One hypothesis that could explain the discrepancy observed between the experimental strain at break values and the EBM prediction is based on the effect of mutual constraint between the phases. In fact, the constraint provided by the surrounding PBS matrix decreased the strain at break of PHBV when it was dispersed in the blend. This effect could not be captured by the EBM model.

The storage modulus (E') and tan δ curves of the PBS, PHBV, and PBS/PHBV blends as a function of the temperature are reported in Figures 8 and 9, respectively. As shown in Figure 8, it over the entire investigated experimental window (from −100 to 100°C), PHBV exhibited higher E' values, whereas PBS showed the lowest E'. This was in line with the elastic modulus data obtained from the tensile test. E' dropped drastically when the temperature reached a range of −30 to −10°C, as the materials were entering the glass–rubbery transition region. As the temperature increased, the polymer chain mobility increased, and the random motion of the molecular chains was enhanced.[33,34] This reduced the rigidity of the material, and

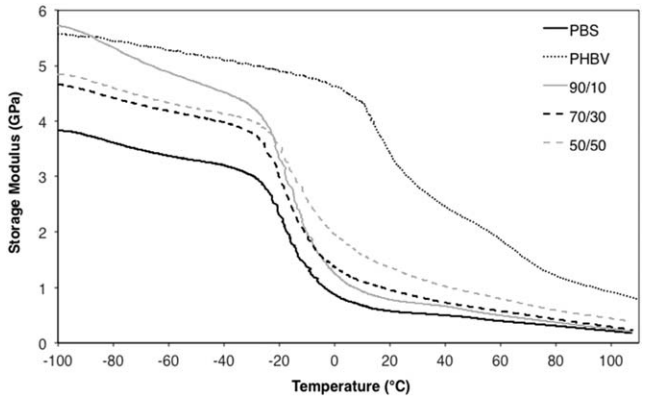

Figure 8. E' values of the PBS, PHBV, and their blends as a function of the temperature.

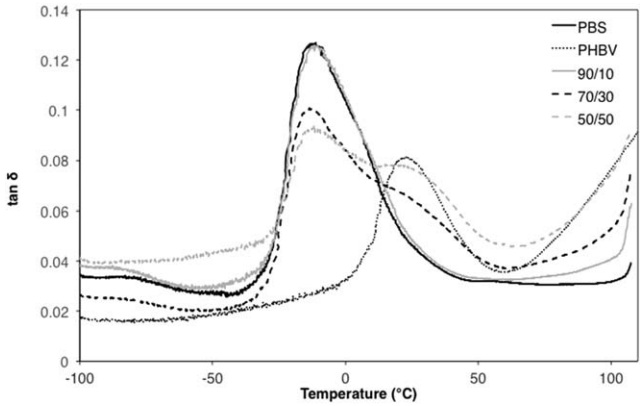

Figure 9. Tan δ of PBS, PHBV, and their blends as a function of the temperature.

thus, E' was greatly decreased. As reported in Figure 10, it was interesting to note that the E' values of the 90 : 10 blend was the highest among all of the blends below T_g. However, E' was drastically reduced in its glass–rubbery transition region and became the lowest among the blends above T_g. A possible reason for this peculiar behavior was the residual stress in the 90 : 10 blend, which may have increase its apparent stiffness. As the temperature increased, the molecular chains assumed a higher mobility, and residual stresses may have been gradually released. Hence, E' dropped as the temperature increased. Above T_g, the results of E' showed a good fit to the tensile modulus.

T_g could be detected as the maximum value of the tan δ peaks reported in Figure 9. In general, T_g as function of the blend composition reflects the miscibility (or immiscibility) of a polymer blend. As a rule of thumb, the observation of a single T_g region in the polymer blends is used as an indication of fully miscible blends. Immiscible polymer blends clearly demonstrate two (or multiple) T_g' s; this correspond to the T_g of each respective component in the blends.[35] Neat PBS showed a T_g at −12°C, and neat PHBV exhibited a T_g of 20°C. Two distinct peaks were apparent in the 70 : 30 and 50 : 50 blends; this indicated the existence of two different transitions, each one very close to the T_g values of PBS and PHBV. Therefore, we concluded that these blends were immiscible. For the 90 : 10 blend, although there was only a single tan δ peak being observed, the blend was believed to be immiscible, as shown in the SEM micrographs. The tan δ peak in the 90 : 10 blend was contributed by the PBS segment, as it showed a T_g that was close to the T_g of neat PBS. We believed that the low content of the PHBV segment in the 90 : 10 blend caused its T_g to be more difficult to detect because of the resolution of the equipment. Moreover, the intensity of the tan δ peak, which corresponded to the PBS amorphous phase (∼−12°C), was greater than the intensity of the tan δ peak, which corresponded to the PHBV amorphous phase (∼20°C). The intensity of the tan δ peak reflected the extent of mobility of the polymer chain segments at this temperature.[36] The high intensity of the 90 : 10 blend indicated a high relaxation of the polymer chains, and more energy was released from the material. This could have been contributed by the release of residual stress in the 90 : 10 blend as well, as mentioned earlier. For the 70 : 30 and 50 : 50 blends, the broadening of the tan δ peak was noticeable. This could have been due to the entanglement of the polymer chains, which restricted the segmental mobility of the polymer chains.[36]

Generally, the processing temperature, rotor speed, and mixing time played a crucial role in the morphological development of polymer blends that were produced with the internal mixer. Knowledge of the upper critical solution temperatures (UCSTs) and lower critical solution temperatures (LCSTs) was important for indicating the phase-separation behavior of a polymer blend at a certain composition and temperature. To date, there is a lack of information on the UCST and LCST of PBS/PHBV blends. As discussed in similar work reported by Hsieh[37] on poly(3-hydroxybutyrate) blends with other aliphatic polyesters such as poly(ethylene succinate), poly(ethylene adipate) and poly(butylene adipate), those blends exhibited UCSTs at 180–221°C, depending on blend composition. This means that the aforementioned blends became miscible at temperatures above 180–221°C. Therefore, it was reasonable to assume that the PBS/PHBV blend also exhibited UCST phase behavior; this meant that a higher mixing temperature may have improved the miscibility of the blend. However, the degradation of PBS and PHBV at high temperatures had to be taken into account as well. Further research on this aspect is needed. On the other hand, we believe that the mixing time and rotor speed had only minor effects on the blend miscibility. Favis[38] studied the effects of the processing parameters on the morphology of polypropylene/polycarbonate blends with an internal mixer. He reported that the most significant particle size deformation and disintegration processes took place within the first 2 min of mixing. After 2 min, the size reduction of the minor phase was very small and did not have much influence on the miscibility. He also stated that polypropylene/polycarbonate blend was insensitive to changes in the rotor speed over a threefold to fourfold range. Scott and Macosko[39] also made a similar conclusion for polystyrene/nylon blends, where the majority of the phase size reduction was found to occur during the first 1.5 min of mixing in an internal mixer. Hence, we expected that the miscibility of

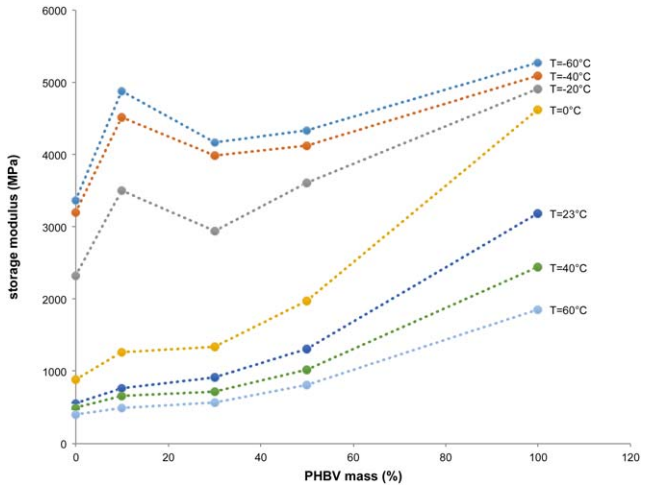

Figure 10. Isothermal E' values [at various temperatures (Ts)] as a function of the blend composition. [Color figure can be viewed in the online issue, which is available at wileyonlinelibrary.com.]

the PBS/PHBV blend would not be affected by changing the current rotor speed (60 rpm) and mixing time (5 min). In short, the mixing temperature played a crucial role in affecting the blend miscibility, and that will be one of the important areas in our future research.

CONCLUSIONS

PBS and PHBV had poor compatibility with each other and formed immiscible blends. This was proven from the observations of distinct phase separations under SEM and the existence of two different T_g's in the blends, as shown by DMTA. This led to poor tensile strength in the blends. However, the moduli of the PBS/PHBV blends were significantly enhanced compared to that of the neat PBS, whereas the elongation at break values of the blends were higher than that of the neat PHBV. This showed that the blending of PBS and PHBV could mitigate their less desirable properties, such as the brittleness of PHBV and the softness of PBS. The EBM was successfully adopted to model the modulus and strength data. From the EBM model, a relatively low A ($A = 0.3$) was estimated. Also, DSC analysis revealed that the blending of PBS and PHBV had positive effects on the crystallization of PBS by increasing the crystallization rate and degree of crystallization. From TGA, we concluded that the interactions of PBS and PHBV molecular chains hindered the degradation of PHBV to a certain degree and increased its thermal stability but reduced the thermal stability of PBS. This suggested that compatibilization was essential for improving the blend compatibility. Furthermore, investigations on the LCST and UCST phase diagrams of the PBS/PHBV blends will be useful for providing a better understanding of the temperature–composition–miscibility relationships of the blends.

ACKNOWLEDGMENTS

One of the authors (Y.J.P.) gratefully acknowledges the financial support of a Universiti Sains Malaysia Research University Cluster Grant (contract grant number 1001/PKT/8640012) and an Erasmus Mundus One More Step Mobility Grant (contract grant number 2011-2581 001-001 EMA2).

APPENDIX A

In a binary blend, we can assume the coexistence of two components (polymers 1 and 2) in volume fractions v_1 and v_2. The EBM schematically depicted in Figure A- operates with the assumption of partly parallel (subscript p) and partly series (subscript s) couplings of components 1 and 2: fractions v_{1p} and v_{2p} form the parallel branch (being coupled in parallel to the acting stress), and fractions v_{1s} and v_{2s} formed the series branch (being coupled in series); these two branches, each consisting of two blocks, are coupled in parallel.

The EBM is a two-parameter model, and of its four volume fractions (v_{ij}), only two are independent. Its volume fractions are interrelated as follows:

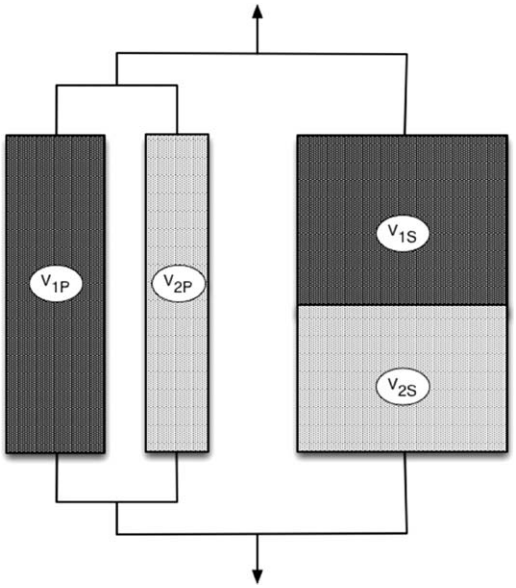

Figure A-1. Graphical representation of an EBM for a 60/40 binary blend.

$$\begin{gathered} v_p = v_{1p} + v_{2p};\ v_s \quad v_{1s} + v_{2s} \\ v_1 = v_{1p} + v_{1s};\quad v_2 = v_{2p} + v_{2s} \\ v_1 + v_2 = v_p + v_s = 1 \end{gathered} \tag{A-1}$$

where v_p and v_s are the total volume fractions of the parallel branch and the series branch, respectively.

The tensile moduli of the parallel (E_p) and series (E_s) branches of the EBM can be computed as follows:[25,26,29]

$$E_p = (E_1 v_{1p} + E_2 v_{2p})/v_p$$
$$E_s = v_s/[(v_{1s}/E_1) + (v_{2s}/E_2)]$$

where E_1 and E_2 are the Young's moduli of the parent phases 1 and 2, respectively.

The resulting tensile modulus of two components blend (E_b) is then given as the sum $E_p v_p + E_s v_s$:

$$E_b = E_1 v_{1p} + E_2 v_{2p} + v_s^2/[(v_{1s}/E_1) + (v_{2s}/E_2)] \tag{A-2}$$

It has been shown that the strength of the binary blend (S_b) can be estimated as follows:[25,26,29,30]

$$S_b = S_1 v_{1p} + S_2 v_{2p} + A S_1 v_s \tag{A-3}$$

where $S_1 < S_2$ characterizes the parent polymers with S_1 and S_2 corresponding to the strength of the parent phases 1 and 2, respectively. Two limiting values of S_b, identified by the lower or upper bound, can be distinguished by means of eq. (A-): (1) interfacial adhesion is so weak that complete debonding occurs before fracture of constituents coupled in series ($A = 0$ at the fracture stress). Consequently, the lower bound of S_b is equal to the sum of the contributions of two parallel elements; (2) interfacial adhesion is strong enough to transmit the acting stress between constituents so that no debonding ($A = 1$) appears in the course of the fracture process, and then, the contribution of the series branch is added to that of the parallel branch. However, if two components differing in strength are coupled in series, the branch yields at S_1 or S_2.

The second step of the outlined scheme is the evaluation of v_{ij}, defined in Figure A-. Percolation theory[40,41] provides a universal formula for the elastic modulus of binary systems where the contribution of the second component is negligible:

$$E_{1b}=E_0(v_1-v_{1cr})^q \quad \text{(A-4a)}$$

where E_0 is a constant, q is the critical exponent,[40] and E_{1b} is the modulus of a single-component blend in which the component 1 assumes the same phase structure as in a blend with another polymer. It has been experimentally shown[26,42] that eq. (A) can plausibly fit the modulus of blends with $E_1 >> E_2$ in the range $v_{1cr} \le v_1 \le 1$ so that the modulus of the neat component 1 can be expressed as follows:

$$E_1=E_0(v_1-v_{1cr})^{q_1}$$

Thus

$$E_{1b}=E_1[(v_1-v_{1cr})/(1-v_{1cr})]^{q_1}$$

If $E_1 >> E_2$, the contribution $E_2\ v_{2p}$ of component 2, which is coupled in parallel, and the contribution of the whole series branch (Figure A-) to the modulus of the EBM are negligible in comparison with the contribution the $E_1\ v_{1p}$ of component 1. Consequently, $E_1\ v_{1p}$ (or $E_2\ v_{2p}$ for $E_2 >> E_1$) can be set equal to E_{1b} (or E_{2b} for $E_2 >> E_1$), that is, $E_{1b} = E_1\ v_{1p}$ and $E_{2b} = E_2\ v_{2p}$. Comparing the latter relations with eq. (4b), we can see that

$$v_{1p}=[(v_1-v_{1cr})/1-v_{1cr}]^{q_1} \quad \text{(A-5a)}$$

$$v_{2p}=[(v_2-v_{2cr})/1-v_{2cr}]^{q_2} \quad \text{(A-5b)}$$

The remaining v_{1s} and v_{2s} are evaluated with eq. (A1). In the marginal zone $0 < v_{1cr} < v_{1cr}$ (or $0 < v_2 < v_{2cr}$), where only component 2 (or 1) is continuous, simplified relations can be used for the minority component, that is, $v_{1p} = 0$ and $v_{1s} = v_1$ (or $v_{2p} = 0$ and $v_{2s} = v_2$), to obtain an approximate prediction of the mechanical properties.

There are many phenomena in physics whose effective behavior is dominated by the connectivity of the system and can be described well by the percolation theory. The percolation theory is a mathematical model of the connectivity of randomly distributed objects in complex geometries. Continuum percolation models form a number of objects randomly distributed within the system; these can freely overlap each other and, consequently, make a cluster of objects. For infinite systems around the percolation threshold, power law equations with q have been proven to effectively model the object distributions. The most ascertained values of q for the percolation of mechanical parameters (modulus, strength, etc.) are located in an interval of 1.6–2.0 so that $q = 1.8$ can be used also as an average value.

For a three-dimensional cubic lattice, the percolation threshold ($v_{cr} = 0.156$) was calculated.[41,43,44] In general, the prediction based on the universal values $v_{1cr} = v_{2cr} = 0.156$ and $q_1 = q_2 = 1.8$ should be viewed as the first approximation that it may not be in good accordance with the experimental data because the real v_{1cr} and v_{2cr} of the polymer blends frequently differ from 0.156 and from each other. On the other hand, if the experimental data on the physical properties of blends are available, the actual values of the parameters can be estimated by a fitting procedure.

REFERENCES

1. Global Industry Analysts. Biodegradable Polymers: A Global Strategic Business Report; Global Industry Analysts: USA, **2012**; p 1–66.
2. Khalil, F.; Galland, S.; Cottaz, A.; Joly, C.; Degraeve, P. *Carbohydr. Polym.* **2014**, *108*, 272.
3. Chieng, B. W.; Ibrahim, N. A.; Yunus, W. M. Z. W. *eXPRESS Polym. Lett.* **2010**, *4*, 404.
4. Okamoto, K.; Ray, S. S.; Okamoto, M. *J. Polym. Sci. Part B: Polym. Phys.* **2003**, *41*, 3160.
5. Xu, J.; Guo, B. H. *Biotechnol. J.* **2010**, *5*, 1149.
6. Avella, M.; Rota, G. L.; Martuscelli, E.; Raimo, M.; Sadocco, P.; Elegir, G.; Riva, R. J. *Mater. Sci.* **2000**, *35*, 829.
7. Srithep, Y.; Effingham, T.; Peng, J.; Sabo, R.; Clemons, C.; Turng, L. S.; Pilla, S. *Polym. Degrad. Stab.* **2013**, *98*, 1439.
8. Liu, Q. S.; Zhu, M. F.; Chen, Y. M. *Polym. Int.* **2010**, *59*, 842.
9. Vroman, I.; Tighzert, L. *Materials* **2009**, *2*, 307.
10. Lim, J. S.; Noda, I.; Im, S. S. *Eur. Polym. J.* **2008**, *44*, 1428.
11. Ma, P. M.; Hristova-Bogaerds, D. G.; Lemstra, P. J.; Zhang, Y.; Wang, S. F. *Macromol. Mater. Eng.* **2012**, *297*, 402.
12. Qiu, Z. B.; Ikehara, T.; Nishi, T. *Polymer* **2003**, *44*, 2503.
13. Zhu, W. F.; Wang, X. J.; Chen, X. Y.; Xu, K. T. *J. Appl. Polym. Sci.* **2009**, *114*, 3923.
14. Ma, P.; Cai, X.; Wang, W.; Duan, F.; Shi, D.; Lemstra, P. J. *J. Appl. Polym. Sci.* **2014**, *131*, 41020.
15. Qiu, Z.; Ikehara, T.; Nishi, T. *Polymer* **2003**, *44*, 7519.
16. Campoy, I.; Gómez, M. A.; Marco, C. *Polymer* **1998**, *39*, 6279.
17. Correlo, V. M.; Boesel, L. F.; Bhattacharya, M.; Mano, J. F.; Neves, N. M.; Reis, R. L. *Mater. Sci. Eng. A* **2005**, *403*, 57.
18. Wang, X.; Chen, Z.; Chen, X.; Pan, J.; Xu, K. *J. Appl. Polym. Sci.* **2010**, *117*, 838.
19. Jud, K.; Kausch, H. H.; Williams, J. G. *J. Mater. Sci.* **1981**, *16*, 204.
20. Zhang, X.-M.; Yin, Z.; Song, Y.; Yin, J. *Chin. J. Polym. Sci.* **1999**, *17*, 237.
21. Qiu, Z. B.; Ikehara, T.; Nishi, T. *Polymer* **2003**, *44*, 7519.
22. Buxton, G. A.; Balazs, A. C. *Mol. Simul.* **2004**, *30*, 249.
23. Mittal, V. Functional Polymer Blends: Synthesis, Properties, and Performance; Taylor & Francis: USA, **2012**; p 156.
24. Kolarik, J. *Polymer* **1994**, *35*, 3631.
25. Kolarik, J. *Polym. Networks Blends* **1995**, *5*, 87.

26. Kolarik, J. *Polym. Eng. Sci.* **1996**, *36*, 2518.
27. Kolarik, J. *Polymer* **1996**, *37*, 887.
28. Kolarik, J. *Polym. Compos.* **1997**, *18*, 433.
29. Kolarik, J. *Eur. Polym. J.* **1998**, *34*, 585.
30. Kolarik, J. *J. Macromol. Sci. Phys. B* **2000**, *39*, 53.
31. Kolarik, J.; Pegoretti, A.; Fambri, L.; Penati, A. *J. Polym. Res. Taiwan* **2000**, *7*, 7.
32. Phua, Y. J.; Chow, W. S.; Mohd Ishak, Z. A. *eXPRESS Polym. Lett.* **2013**, *7*, 340.
33. Bikiaris, D.; Prinos, J.; Botev, M.; Betchev, C.; Panayiotou, C. *J. Appl. Polym. Sci.* **2004**, *93*, 726.
34. Roth, C. B.; Dutcher, J. R. *J. Electroanal. Chem.* **2005**, *584*, 13.
35. Kalogeras, I. M.; Brostow, W. *J. Polym. Sci. Part B: Polym. Phys.* **2009**, *47*, 80.
36. Hill, D. J. T.; Perera, M. C. S.; Pomery, P. J.; Toh, H. K. *Polymer* **2000**, *41*, 9131.
37. Hsieh, Y. T.; Woo, E. M. *eXPRESS Polym. Lett.* **2011**, *5*, 570.
38. Favis, B. D. *J. Appl. Polym. Sci.* **1990**, *39*, 285.
39. Scott, C. E.; Macosko, C. W. *Polymer* **1995**, *36*, 461.
40. de Gennes, P. G.; Pincus, P.; Velasco, R. M.; Brochard, F. *J. Phys. (Paris)* **1976**, *37*, 1461.
41. Hsu, W. Y.; Wu, S. H. *Polym. Eng. Sci.* **1993**, *33*, 293.
42. Lyngaae-Jorgensen, J.; Kuta, A.; Sondergaard, K.; Poulsen, K. V. *Polym. Networks Blends* **1993**, *3*, 1.
43. Sax, J.; Ottino, J. M. *Polym. Eng. Sci.* **1983**, *23*, 165.
44. Utracki, L. A. *J. Rheology* **1991**, *35*, 1615.